scientific reports

Check for updates

OPEN

Integrating ontogenetic and behavioral analysis in fossil and extant *Lynx pardinus* (Temminck, 1827)

Israel Jesus Jimenez[1,2], Rebeca García-González[3], Montserrat Sanz[4], Joan Daura[4], Ignacio de Gaspar[2,5], María Isabel García-Real[2,6] & Nuria García[1,2,7]✉

This study proposes new developmental stages for age classification of the Iberian lynx (*Lynx pardinus*), based on tooth development observed through X-rays, with a focus on juveniles. The classification defines a set of developmental markers expected as a cub grows, identifying five age categories: neonate, two juvenile stages, subadult, and adult. As an alternative methodology, we adapted pulp cavity infilling analyses previously applied in other carnivores, estimating development stages with ordinal logistic regression equations that examine root development in the lower and upper carnassial. These methods were then applied to fossil samples to interpret the age and behaviour of past lynx populations at Terrasses de la Riera dels Canyars (TC) and Cova del Gegant (CG). The results at TC suggest a minimum of 16 individuals, with a mortality profile suggesting a living structure population. In contrast, the CG mortality profile align closely with to seasonal mortality profiles, reinforcing previous assumptions denning activity. The regression-based age estimation proved effective for both modern and fossil samples, supporting its potential use in conservation and reintroduction. Additionally, this ontogenetic approach provides comprehensive mortality profiles and insights into the behavioural history of *L. pardinus*.

Keywords *L. pardinus*, Pleistocene, Cubs, Ontogeny, Den, prediction model

The Iberian or pardel lynx (*Lynx pardinus* Temminck, 1827) is a feline species native to the Iberian Peninsula[1]. At the beginning of the 2000s, *L. pardinus* was one of the most endangered mammal species globally with fewer than 100 individuals remaining in southern Spain (Doñana, Huelva, Spain)[2] and it was classified as Critically Endangered[1]. Nevertheless, after intensive conservation programs, the population has recovered over the last few years[3]. Nowadays, the population overs 1600 individuals, spreading across Spain and Portugal[4]. However, during the Upper Pleistocene and early Holocene, its distribution included the entire Iberian Peninsula, south-eastern France and Italy, inhabiting wide-ranging ecosystems from which it is now restricted[5–7].

L. pardinus is a solitary and territorial animal[8], distinguished by its sleek appearance, long limbs, small head, and very short tail[9]. This species exhibits sexual dimorphism[10], with males being larger and heavier than females. It is primarily crepuscular and nocturnal[11], relying almost exclusively on rabbits for sustenance, which make up 85–99% of its diet[12,13]. Females reach sexual maturity at around two years of age[14,15]. Breeding is seasonal, with oestrus occurring in winter, mainly in January and February, and gestation lasting between 63 and 66 days[16,17]. Most births occur between March and April[18], with litters typically consisting of three to four cubs[19]. At birth, the offspring are considered semi-altricial and require substantial maternal care[20].

Dental development begins around the third week of life. The first teeth to erupt are the upper canines, which appear at approximately 17 days (within a range of 14–19 days), followed shortly by the lower canines at around 19 days (16–24 days). The upper and lower incisors emerge around 19–20 days (16–26 days), while premolars

[1]Departamento de Geodinámica, Estratigrafía y Paleontología, Facultad de Ciencias Geológicas, Universidad Complutense de Madrid, Madrid, Spain. [2]Grupo UCM Ecosistemas Cuaternarios, Universidad Complutense de Madrid, Madrid, Spain. [3]Laboratorio de Evolución Humana, Universidad de Burgos, Burgos, Spain. [4]Dept. d'Història i Arqueologia, Grup de Recerca del Quaternari (GRQ) -SERP, Universitat de Barcelona, Barcelona, Spain. [5]Departamento de Anatomía y Embriología, Facultad de Veterinaria, Universidad Complutense de Madrid, Madrid, Spain. [6]Departamento de Medicina y Cirugía Animal. Facultad de Veterinaria, Universidad Complutense de Madrid, Madrid, Spain. [7]Centro Mixto UCM-ISCIII de Evolución y Comportamiento Humanos, Madrid, Spain. ✉email: nugarcia@ucm.es

appear between 37 and 38 days (33–40 days). Juveniles remain within the natal territory until dispersal, which occurs between one and two years of age[16]. The lifespan of *L. pardinus* is estimated to be up to 14 years[21].

Carnivorous mammals typically give birth to relative underdeveloped young that need complete care during their early life for survival[22]. Neonates are usually the most vulnerable life stage in mammals[19]. Dens play a crucial role in the development of the young, providing shelter from environmental conditions, optimal ambient conditions for successful development, and protection from predators[23–26]. Females *L. pardinus* give birth in dens knows as natal dens. These spaces are used to rear cubs during their first weeks of life. At around one months old, cubs begin following their mother and leave the natal den, but they continue using another type of den, the auxiliary den, until their mobility is fully developed (around two months of life[18,23]. Ethological studies in deltaic regions without caves, such as the Doñana region, indicate that lynxes usually use hollows in large trees to rear their newborns[23]. However, rocky areas are also suitable for denning[23,27]. This observation seems to be supported by fossil evidence, so lynx remains are commonly recovered in karstic contexts[28,29]. Recent research has shown, using taphonomical criteria, that *L. pardinus* used caves (Cova del Gegant, Sitges, Barcelona, Spain) as a reproductive den[29]. In contrast, other Pleistocene cavities, such as Cova del Coll Verdaguer, were used by lynxes as a refugee for resting, transporting their prey, and feeding on it[28,30,31].

Age estimation is essential for assessing population dynamics, aiding managers in the protection of endangered populations, and providing insights into populations growth and stability (e.g., Refs.[32–34]. Age determination is typically based on dental eruption and replacement, counting visible *cementum annuli*, or analysing the attrition of permanent teeth[35–37]. Although these methods are valuable, they are hindered by certain limitations as they can be influenced by external factors such as environmental conditions. However, it has been demonstrated that dental development[37] is less affected by these biases. Previous studies by Jimenez et al.[38,40] have shown that using X-rays to analyse tooth development is an effective method for determining the age at death in Pleistocene hyena populations. For *L. pardinus*, several studies have focused on cub development. García-Perea[41] proposed five developmental stages based on tooth replacement. While this work includes references to some individuals of known age, the classification is not directly age-correlated, making it challenging to apply for determining the age at death. Yerga[18], and Yerga et al.[42], describes the early development and growth of cubs, though these studies only cover the first two months life. On the other hand, By last, Zapata et al.[21] conducted an age analysis based on counting the *cementum annuli* in canines, but this technique is invasive and requires the destruction of fossils.

The aim of this work is to develop a method for determining the age of lynxes based on teeth, applicable to both modern and fossil specimens, while also enabling behavioural inferences. Here, we apply an ontogenetic classification of *L. pardinus* based on tooth development and eruption/replacement patterns observed through X-rays images, which were correlated to key behavioural milestones of the species. This classification was developed using data from modern *L. pardinus* specimens housed in the Museo de Ciencias Naturales de Madrid (MNCN, Madrid, Spain) and the Estación Biológica de Doñana (EBD-CSIC, Seville, Spain), as well as developmental information on lynx from previous studies[18,21,23,42]. Building on this classification we apply, for the first time in *L. pardinus*, an age estimation technique based on the infilling of pulp cavities in the roots of molars and premolars, a method previously used in other carnivores[43–52]. Specially, we calculated indexes for the upper fourth premolar (P^4 and the lower first molar (m_1), which were used to estimate age at death through predictive equations. Finally, the methodology was applied to two fossil populations that inhabited the Garraf Massif (Barcelona, Spain) during the Upper Pleistocene: Terrasses de la Riera dels Canyars site (Gavà, Spain) and Cova del Gegant (Sitges, Spain), a region characterized by rocky terrain[29,53].

Results

Closure of pulp cavity in extant specimens

In extant specimens, the indexes were obtained for the distal root of P^4, and mesial and distal root of m_1 ($n = 28$) (Table 1). These specimens were assigned to 5 categories of development (Fig. 1) resulting from analysing lynx collections from EBD and MNCN, together with descriptions of *Lynx* development by previous authors[18,21,23,42] (see Methods section for detailed description of the stages). No indexes were recorded for Stage A, as the carnassial teeth are still within the alveolar sac and crowns are not yet defined. Figure 2 illustrates the relationship between the stage and index for each age category in the distal root of P^4 and mesial and distal root of m_1 in a box plot (summary statistics for the indexes of each stage are provided in Supplementary Table S1).

- Distal root of P^4 (Fig. 2a): An overlap is observed between samples with the lowest index values of a given stage and those with the highest index values of the subsequent stage. Samples corresponding to Stage B (youngest individuals) exhibit the highest index values, while samples of Stage C (sub-adult to adult individuals) have the lowest index values. As the stages (i.e., age) increase, the index value decreases, indicating an inverse relationship between the two variables. The Spearman's correlation between indexes and stages of development is significant ($p < 0.05$) and very high ($r = -0.90$), highlighting a strong negative relationship between the stages and the index values.
- Mesial root of m_1 (Fig. 2b): The box plot reveals a distribution of samples similar to that observed in the distal root of the P^4. The relationship between stages and indexes appears to be negative, with index values decreasing as stages increase. As in the previous case, some overlap is observed between samples. The Spearman's rank correlation between indexes and stages is significant ($p < 0.05$), negative and very high ($r = -0.91$).
- Distal root of m_1 (Fig. 2c): With exception of Stage B, the maximum and minimum index values are very closed across the remaining stages, indicating low variance in the indexes of the samples, as shown in the box plot. Again, the relationship between the stages and index values appears to be negative, with index as stages increase. Spearman's rank correlation indicates a very strong negative relation between stages and indexes ($r = -0.95$) and significant ($p < 0.05$).

Sample	Stage (y)	Distal root P^4 Index (x)	Mesial root m_1 Index (x)	Distal root m_1 Index (x)
EBD-25,375 M	A	–	–	–
EBD-27,759 M	A	–	–	–
EBD-29,923 M	A	–	–	–
EBD-29,981 M	A	–	–	–
EBD-29,982 M	A	–	–	–
EBD-6975 M	B	0.85	0.87	0.25
EBD-19,322 M	B	0.82	0.83	0.10
EBD-29,893 M	B	0.88	0.87	0.14
EBD-30,096 M	B	0.88	0.85	0.16
MNCN-16,785	B	–	0.82	0.1
MNCN-16,755	B	–	0.84	0.17
MNCN-1677 A	B	–	0.88	0.2
MNCN-1677B	B	–	0.72	0.17
MNCN-16,778 A	B	–	0.82	0.15
MNCN-16778B	B	–	0.86	–
MNCN-16,783	B	0.89	0.86	0.16
EBD-1376 M	C	0.77	0.76	0.06
EBD-19,283 M	C	0.78	0.79	0.08
EBD-19,319 M	C	0.76	0.78	0.08
EBD-19,794 M	C	0.49	0.59	0.09
EBD-26,314 M	C	–	0.74	0.09
EBD-27,761 M	C	0.8	0.8	0.1
EBD-30,111 M	C	0.73	0.71	0.05
EBD-30,112 M	C	0.66	0.68	0.08
MNCN-16,791	C	0.83	0.79	0.07
MNCN-16,794 A	C	0.54	0.67	0.06
MNCN-16794B	C	–	0.67	0.07
MNCN-16,788 A	C	0.83	0.79	0.07
MNCN-16788B	C	–	0.82	–
EBD-1400 M	D	0.57	0.49	0.03
EBD-5955 M	D	0.53	0.6	0.02
EBD-7099 M	D	0.4	0.32	0.03
EBD-26,315 M	D	–	0.46	0.02
EBD-30,100 M	D	0.46	0.39	0.02
MNCN-16,799	D	0.55	–	–
EBD-29,995 M	E	0.35	0.32	0.02
EBD-29,999 M	E	0.31	0.24	0.02
EBD-30,090 M	E	–	0.35	0.01
EBD-30,183 M	E	0.25	0.18	0.01
EBD-30,256 M	E	0.39	0.3	0.02
EBD-30,298 M	E	0.41	0.28	0.02

Table 1. Stages of development of the specimens ($n = 28$) based on tooth development classification and pulp cavity ratio (indexes) for each analysed root. Specimens with known age at death are highlighted in grey.

Age model: ordinal logistic regression

The ordinal logistic regression allowed us to predict stage of development based on index values. We obtained a coefficient of $x = -42.61$ for the distal root of P^4 ($n = 25$) (Table 2). The intercepts (mean ± SE) obtained were as follows: for B/C, -35.53 ± 12.86; for C/D, -26.41 ± 9.82; and for D/E, -17.45 ± 6.26 (Supplementary Table S1). The equation provides the probability at which transitions between stages occur in the distal root of P^4. Specimens with index values above 0.72 are classified as Stage B, those with values between 0.72 and 0.57 fall into Stage C, specimens with index values between 0.57 and 0.39 are assigned to Stage D, and finally, those with index values below 0.39 are classified as Stage E. Table 2 presents the application of the prediction model on extant specimen samples. The prediction results indicate high accuracy for the distal root of P^4, with a correct classification rate of 80%. Fitted probabilities, which represent the estimated likelihood that an observation falls into a specific ordinal category based on the model's independent variables, are also displayed in Table 3. For this

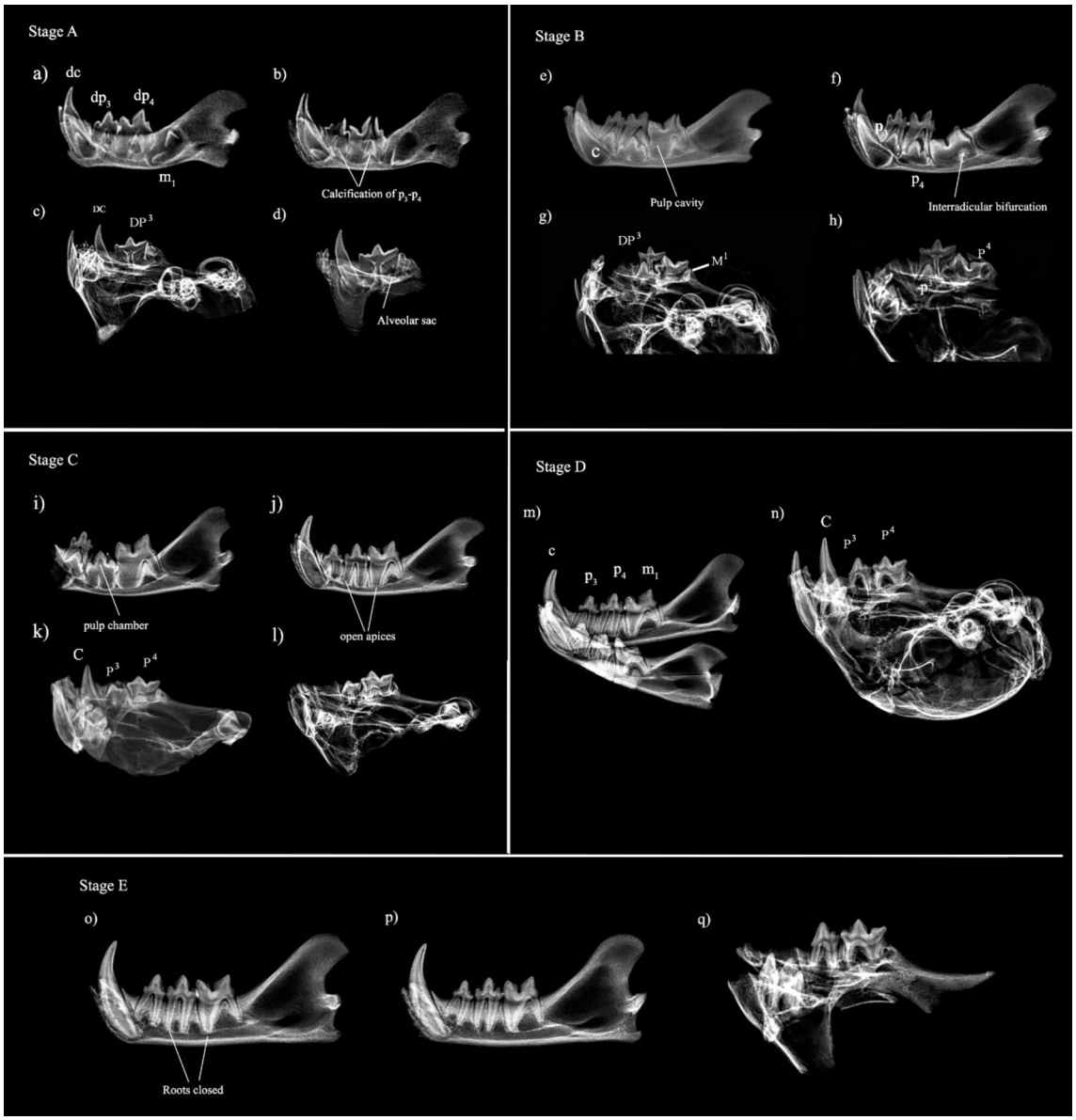

Fig. 1. Radiograph showing extant *Lynx pardinus* specimens from EBD and MNCN. Stage A: (**a**) Hemimandible EBD-27,759 M; (**b**) Hemimandible EBD-29,923 M; (**c**) Maxilla EBD-29,981 M; (**d**) Maxilla EBD-27,759 M. Stage B: (**e**) MNCN-16,783; (**f**) EBD-30,096 M; (**g**) EBD-19,322 M; (**h**) EBD-29,893 M. Stage C: (**i**) EBD-27,761 M; (**j**) EBD-30,111 M; (**k**) MNCN-16,791; (**l**) EBD-1376 M. Stage D: (**m**) EBD-1400 M; (**n**) EBD-30,100 M. Stage E: (**o**) EBD-29,995 M; (**p**) EBD-30,183 M; (**q**) EBD-29,999 M. All radiographs of maxillae and hemimandibles used in this study (categorised by age) can be found in the Supplementary Material. All images have been procedes using software Radiant Dicom Viewer (Medixant. RadiAnt DICOM Viewer, Version 2021.1. Jun 27, 2021. URL: https://www.radiantviewer.com).

initial model, out of the 25 specimens analysed, the model misclassified 5 specimens: one in Stage B, two in Stage C, and one each in Stages D and E, respectively.

For mesial root of m_1 we obtained a coefficient of $x = -42.63$, and intercepts were for B/C, -34.33 ± 11.40; for C/D, -25.19 ± 8.60, for D/E, -14.84 ± 4.81 ($n = 35$, Table 2). The predictive equation shows the following critical values:

Indexes higher than 0.70 are classified in Stabe B. Indexes with values between 0.70 and 0.59 are classified in Stage C. Indexes between 0.59 and 0.34 are classified in Stage D. Finally, indexes with values below 0.34 are classified in Stage E. In Table 2, we can observe the results of the prediction model. The results indicate a correct classification rate of 82.6%, being more accurate than the model of distal root of P^4. For mesial root of m_1 model, out of the 35 specimens analysed, 6 specimens were misclassified: one in Stage B, two in Stage C, two in Stages D and one in Stage E.

Regarding the distal root of m_1, the model could not be applied ($n = 34$, see Supplementary material). In this case, the algorithm indicates perfect separation between some stages, so model cannot predict on them. Here,

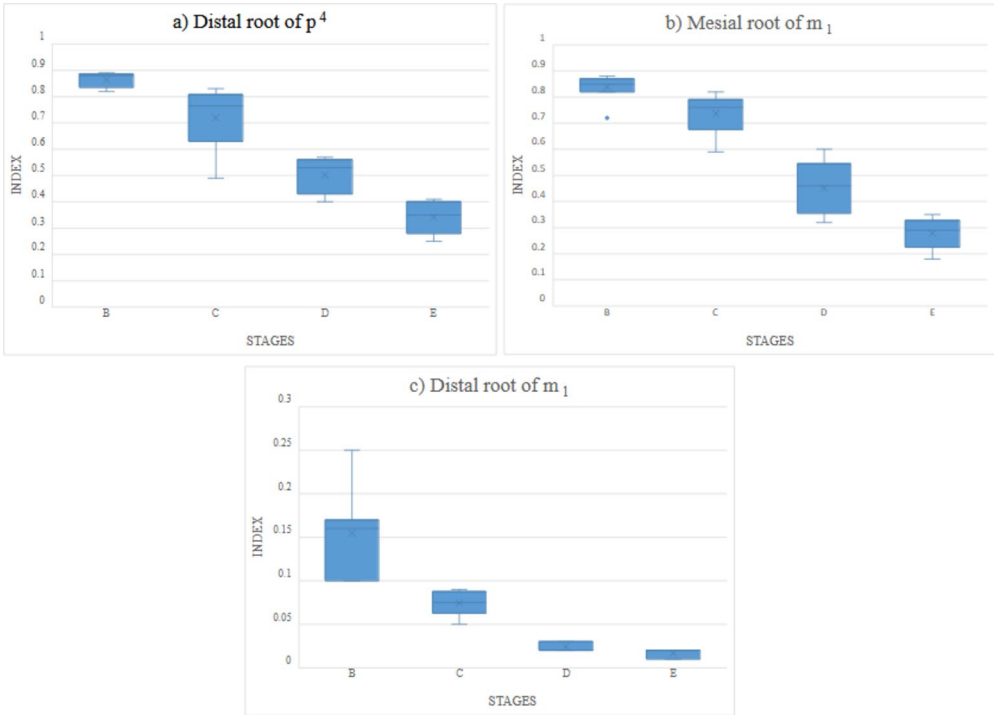

Fig. 2. Box plots showing the relation between the indexes (y) and the stages of development (x). (**a**) Distal root of P^4; (**b**) Mesial root of m_1; (**c**) Distal root of m_1.

	Distal root of P^4 ($n=25$)				Mesial root of m_1 ($n=35$)			
	Value ($p<0.05$)	Standard Error	t value	Critical values	Value ($p<0.05$)	Standard Error	t value	Critical values
Coefficient (x)	− 42.61	15.46	− 2.756		− 42.63	14.05	− 3.033	
Intercept B/C	− 35.53	12.86	− 2.762	0.72	− 34.33	11.40	− 3.011	0.7
Intercept C/D	− 26.41	9.82	− 2.688	0.57	− 25.19	8.60	− 2.928	0.59
Intercept D/E	− 17.45	6.26	− 2.786	0.39	− 14.84	4.81	-3.082	0.34

Table 2. Values resulting from the model. Critical values are applied to set the boundary between each stage of development.

we consider suitable to use the maximum and minimum values for index showed in Supplementary table S2 to classified individuals. Thus, those specimens with index values ranging from 0.25 to 0.1 are classified in Stage B. Those, whose indexes range from 0.09 to 0.05 correspond to the Stage C. Indexes between 0.03 and 0.2 are classified in Stage D, and finally, specimens with index values below 0.02 are classified in Stage E.

Analysis of the fossil assemblage

We determined the Minimum Number of Individuals (MNI) for the cranial material from TC and CG. Adult individuals were classified based on the carnassial teeth P^4 and m_1. Neonate individuals were classified according to the developmental stage of dp_4 and DP^3. Subsequently, the ontogenetic classification was compared by analysing the root thickness of the carnassial teeth. The Number of Identified Specimens (NISP) analysed from TC is 44, resulting in a MNI of 16. Among these 16 individuals, 11 are classified as adults, 1 as a neonate, 3 as juveniles, and 1 as a subadult, as shown in the mortality profile (Fig. 3a). The age structure for TC indicates the highest representation in Stage E (adults), comprising 68.6% of the individuals. The next most represented group is Stage B (juveniles) with 12.5%. Stage A (neonates), C (juveniles), and D (subadults) are equally represented in the assemblage, each with 6.3% (Table 4). When indexes for pulp cavity thickness in P^4 and m_1 were calculated and subjected to critical values (B = > 0.70; C = 0.70–0.59; D = 0.59–0.34; and E = < 0.34, for the distal root of p^4; B = > 0.72; C = 0.72–0.57; D = 0.57–0.39; and E = < 0.39, for the mesial root of m_1), the predicted stage aligned with the classification derived from tooth development (Supplementary Table S4). The NISP for CG is 11, corresponding to an MNI of 7 (Table 4). The mortality profile (Fig. 3b) shows that these 7 individuals are distributed as follows: 5 adult individuals (Stage E), 1 neonate (Stage A), and 1 juvenile (Stage C). No specimens were assigned to Stage B or D. The age distribution (Table 4) indicates that the most individuals belong to Stage E (71.4.%), with the remaining categories in the fossil assemblage, Stage A and C, each accounting for 14.3%. As

Sample	Distal root of P^4			Mesial root of m_1		
	Stage	Prediction	Fit. Prob.	Stage	Prediction	Fit. Prob
EBD-6975 M	B	B	0.66	B	B	0.94
EBD-19,322 M	B	C	0.64	B	B	0.74
EBD-29,893 M	B	B	0.87	B	B	0.94
EBD-30,096 M	B	B	0.87	B	B	0.87
MNCN-16,785	–	–	–	B	B	0.65
MNCN-16,755	–	–	–	B	B	0.81
MNCN-16,777 A	–	–	–	B	B	0.96
MNCN-16777B	–	–	–	B	C	0.97
MNCN-16,778 A	–	–	–	B	B	0.65
MNCN-16778B	–	–	–	B	B	0.91
MNCN-16,783	B	B	0.96	B	B	0.91
EBD-1376 M	C	C	0.93	C	C	0.87
EBD-19,283 M	C	C	0.90	C	C	0.65
EBD-19,319 M	C	C	0.95	C	C	0.74
EBD-19,794 M	C	C	0.94	C	D	0.51
EBD-26,314 M	–	–	–	C	C	0.94
EBD-27,761 M	C	C	0.80	C	C	0.55
EBD-30,111 M	C	C	0.97	C	C	0.97
EBD-30,112 M	C	C	0.84	C	C	0.97
MNCN-16,791	C	C	0.54	C	C	0.65
MNCN-16,794 A	C	D	0.69	C	C	0.96
MNCN-16794B	–	–	–	C	C	0.96
MNCN-16,788 A	C	C	0.54	C	C	0.65
MNCN-16788B	–	–	–	C	B	0.65
EBD-1400 M	D	D	0.94	D	D	0.98
EBD-5955 M	D	D	0.97	D	C	0.59
EBD-7099 M	D	E	0.77	D	E	0.76
EBD-26,315 M	–	–	–	D	D	0.98
EBD-30,100 M	D	D	0.89	D	D	0.85
MNCN-16,799	D	E	0.84	-	-	-
EBD-29,995 M	E	E	0.92	E	E	0.76
EBD-29,999 M	E	E	0.98	E	E	0.99
EBD-30,090 M	–	–	–	E	D	0.51
EBD-30,183 M	E	E	0.99	E	E	0.99
EBD-30,256 M	E	E	0.69	E	E	0.88
EBD-30,298 M	E	D	0.50	E	E	0.94

Table 3. Stages based on tooth development, stages predicted by indexes, and the percentage (fitted probability) assigned to each stage. Stage where the model fails in the prediction (with the probability in percentage) are marked in grey.

with the TC specimens, applying critical values to the calculated indexes produced classifications consistent with those previously determined through tooth development analysis (Supplementary Table S4).

Discussion

L. pardinus ontogenetic description

Age estimation is critical for understanding extant population dynamics and for supporting conservation managers in the preservation of wild populations[35]. Furthermore, it is a widely used and valuable tool for inferring ancient behaviour in fossils assemblages[54,55]. For *L. pardinus*, several studies have focused on cub development analysing tooth replacement and *cementum annuli* counting[18,21,41,42]. The estimation of age in *L. pardinus* remains challenging due to methodological limitations. While developmental stages proposed[18,42] based on tooth replacement provide insights, their lack of age correlation limits their utility in mortality analyses. Regarding *cementum annuli* counting, it offers precise results but involve destructive techniques, raising concerns for fossil preservation. These limitations highlight the need for non-invasive, accurate approaches in age estimation.

These previous works support the conception of the age categories presented here, while they provide data on developmental stages at specific ages of lynx individuals. For instance, García-Perea[41], described the state of development of a 6 month old specimen, in which dp_4 was absent, m_1 had completed its eruption, and the lower

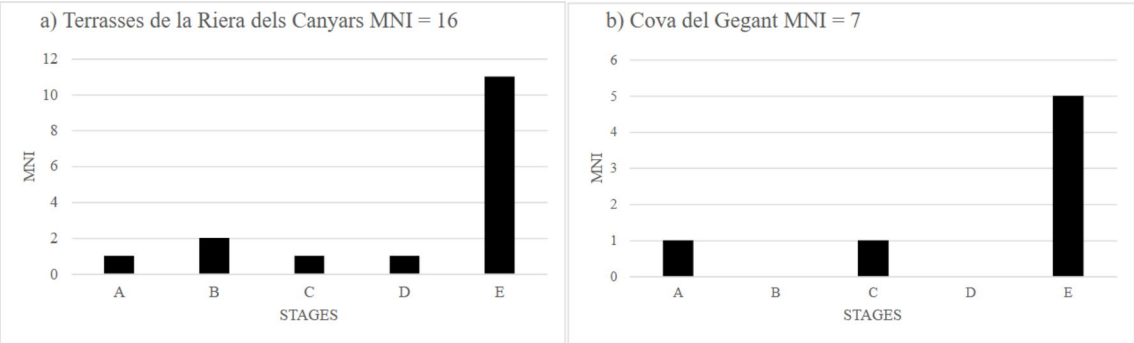

Fig. 3. Age profile of the Terrasses de la Riera dels Canyars (**a**), and Cova del Gegant (**b**) *L. pardinus* populations calculated as percentage minimum number of individuals (MNI). Stage A corresponds to neonate individuals. Stage B and C correspond to juvenile individuals. Stage C corresponds to subadult individuals. Stage E corresponds to adult individuals.

	Isolated dentition					m_1 *and* P^4 in situ					
	dp_4 right	m_1 right	m_1 left	P^4 right	P^4 left	Hemimand right	Hemimand left	Maxi right	Maxi left	NISP (%)	MNI (%)
Terrasses de la Riera dels Canyars											
Stage A	0	0	0	0	0	1	0	0	0	1 (2.3)	1 (6.3)
Stage B	1	0	0	0	1	2	0	0	1	5 (11.3)	2 (12.5)
Stage C	0	0	0	0	0	0	1	0	0	1 (2.3)	1 (6.3)
Stage D	0	0	0	1	0	0	0	0	1	2 (4.5)	1 (6.3)
Stage E	0	2	1	2	2	9	9	6	4	35 (79.5)	11 (68.6)
Total	**1**	**2**	**1**	**3**	**3**	**12**	**10**	**6**	**6**	**44 (100)**	**16 (100)**
Cova del Gegant											
Stage A	0	0	0	0	0	0	0	0	1	1 (9.1)	1 (14.3)
Stage B	0	0	0	0	0	0	0	0	0	0	0
Stage C	0	0	0	1	0	0	1	0	0	2 (18.2)	1 (14.3)
Stage D	0	0	0	0	0	0	0	0	0	0	0
Stage E	0	0	2	0	0	3	2	1	0	8 (72.7)	5 (71.4)
Total	**0**	**0**	**2**	**1**	**0**	**3**	**3**	**1**	**1**	**11 (100)**	**7 (100)**

Table 4. NISP and MNI of *L. pardinus* populations from terrasses de La Riera Dels Canyars and Cova Del Gegant by age categories.

p_4 was erupting. Another specimen, aged between 6 and 8 months, exhibited an already erupted p_4 and the beginning of p_3 eruption. These observations align with our analysis of specimens of known age (EBD-30112 M, 6 months; and EBD-30111 M, 7 months).

The timing of deciduous teeth eruption was straightforward to approach. Fernández and Palomares[23], and Yerga et al.[42] reported that this milestone occurs around the first month of life (up to 40 days old following Yerga et al.[42]. Our analysis of three specimens of known age within this range (EBD-25375 M, 4 weeks of life, EBD-29981 M, 1 month old, and EBD-29982 M: 2 months old) corroborates these early works.

One of the main challenges in this classification was determining the onset of dental replacement. Although precise data on this milestone in cub development are lacking, our observations (EBD-29893 M, 4 months old and EBD-31112 M, 6 months old) suggest that the replacement period begins at the end of the carnassial teeth eruption, at approximately 5 months of age. The specimen EBD-29,893 M shows the m_1 erupting, with premolar crowns still developing. The specimen EBD-30,112 M shows the fully m_1 erupted and the main and distal secondary cups of the p_4 crowns are situated above the gingival margin. In other species of genus *Lynx*, such as *Lynx rufus*, dental replacement starts at the age of 5 months[55], whereas in *Lynx lynx*[57], it begins around 6 months. In these species, tooth replacement begins after the completion of the m_1 eruption process. Based on this information, we set the onset of dental replacement in the *L. pardinus* at 5 months of age.

On the other hand, García-Perea[41] establishes that permanent teeth eruption ends in the *Lynx* genus at 10 months of age. While this occurs at 10 months in *L. lynx*[41,57], it occurs slightly earlier in the bobcat, at 8 months. Our observations are consistent with García-Perea's[41] conclusions, wherein the end of eruption is set around 10 months of age. Subsequently, between 12 and 18 months, the apical foramen of the canine closes, according to Zapata et al.[21].

These frameworks provide basis for defining the ontogenetic categories applied in this study, which correspond to key behavioural milestones of *L. pardinus* (Fig. 4). The first category (Stage A) represents neonates or infants.

During this stage, cubs are sheltered in natal dens by their mothers. By the second month, the cubs begin to walk and explore their surroundings, moving to auxiliary dens[23]. The changes experienced during the first 2 months of life enable cubs to acquire basic physical skills required for to interacting with their environment[42]. This stage concludes with weaning, which typically occurs at the end of the tenth week (around 2 months), coinciding with the completion of tooth eruption[18,42]. Stage B corresponds to cubs venturing out of the den. During this phase, they begin consuming solid food and accompany their mother on short excursions, observing and learning hunting strategies, though they do not actively participate[14,18,42]. Stage C marks a period where cubs follow their mother during daily movements and gradually develop the ability to hunt independently. This stage is also characterised by the onset of nutritional independence, as cubs spending more time away from their mother, while remaining within the natal territory[14]. Stage D corresponds to cubs transitioning to subadults. A period defined by behavioural changes such as the breaking of the maternal bond and preparation for dispersal[14,16]. Stage E corresponds to the transition from subadult to adult, marked by the attainment of sexual maturity. Females typically reach sexual maturity around 24 months, whereas males achieve this milestone at 36 months[14,15].

Analysis of pulp cavity closure

The analysis of pulp cavity closure has been previously applied to carnivores, especially in extant specimens such as black bears[58] (*Ursus americanus* Pallas, 1780), wild cats[50] (*Felis silvestris* Schreber, 1777), foxes[52] (*Vulpes vulpes* Linnaeus, 1758), coyotes[44] (*Canis latrans* Say, 1823), wolve[45,48,48,51] (*Canis lupus* Linnaeus, 1758), or dogs[43,46,47] (*Canis familiaris* Linnaeus, 1758). Binder et al.[59] analysed pulp cavity widths in canines of dire wolf, demonstrating the feasibility of applying it in fossils specimens. Later, Nomokonova et al.[47] adapted the previous methods to the lower canine and carnassial (m_1) in dogs, proving it suitable for age estimation using this tooth as well in archaeological samples.

In this study, we focus for the first time on the lower and upper carnassial teeth of *L. pardinus*. This approach offers an alternative to the classical classification method based on tooth development observations. The results of Spearman's rank correlation reveal a very strong and statistically significant negative relationship between the indexes and developmental stages. This indicates that the index is a reliable tool for estimating developmental stage in *L. pardinus*. Using ordinal logistic regression, we prove a robust predictive methodology for classifying extant specimens of *L. pardinus*. Just by using an isolated tooth (P^4 or m_1), we can successfully classify specimens without relying on the complete dental series. We propose critical values that could be used to classify independent samples based on the pulp cavity filling of the m_1 and P^4. While previous studies applied linear

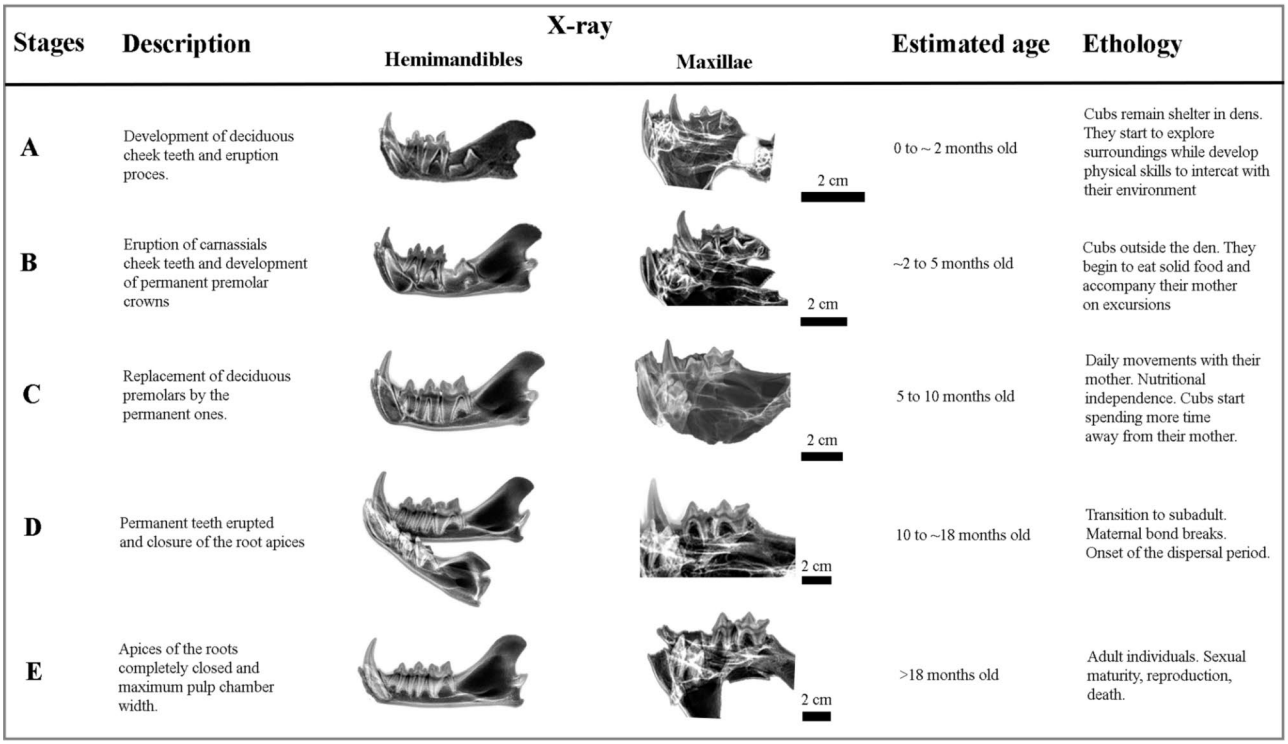

Fig. 4. Summary of the age categories proposed based on tooth development and replacement sequences in extant *Lynx pardinus*. Hemimandible corresponding to Stage A: EBD-29,982 M; Stage B: EBD-30,096 M; Stage C: EBD-30,111 M; Stage D: EBD-1400 M; Stage E: EBD-30,183 M. All hemimandibles are shown in labial view. Maxillae corresponding to Stage A: EBD-29,981 M; Stage B: EBD-30,096 M; Stage C: MNCN-16,788; Stage D: EBD-30,100 M; Stage E: EBD-29,999 M. All maxillae are shown in mediolateral view. All images have been procedes using software Radiant Dicom Viewer (Medixant. RadiAnt DICOM Viewer, Version 2021.1. Jun 27, 2021. URL: https://www.radiantviewer.com).

regressions to estimate age in carnivores, as cited earlier, those employ linear regressions, which perform well when analysing two continuous variables. In contrast, for age ranges, where age categories encompass several months, the ordinal logistic regression model shows high predictive accuracy: 80% for the distal root of the P^4 and 82.6% for the mesial root of the m_1. When misclassification occurs, the model predicts an adjacent stage. This is reasonable, as these specimens had index values near the critical boundaries defining the stages, making them more prone to errors. For the distal root of the m1, we propose using directly age ranges (minimum and maximum) to classify specimens. The model could not be applied to this case for several possible reasons. For instance, the predictor variables might perfectly predict the separation between stages, or there might be limited variability in the indexes within specific stages. Additionally, we observed that pulp cavity filling occurs earlier in the distal root than in the mesial root (Stage D). This is likely due to distal root's narrower anatomical structure, which results in reduced variability in the index values.

Palaeocological implications in fossil assemblages

The presence in sites of deciduous teeth, and therefore juveniles, has generally been associated with denning activity. However, in some carnivore species, juveniles leave the den before the replacement of deciduous teeth[18,60–64]. Consequently, if the developmental stages of juveniles associated with denning behaviour are not considered, it may lead to misinterpretation of the site.

The MNI obtained for the TC site is 16, 3 more than in estimates[53]. This increase suggests that the proposed methodology provides a more accurate approach to MNI estimations in archaeological contexts. The site contains a high number of adult individuals, which are by far the most represented group in the assemblage (11 individuals). Moreover, all developmental stages are present in the mortality profile. The presence of Stage A cubs could suggest the presence of dens (both natal and auxiliary) in the area, as indicated previous studies at the site[53,65]. In the same way, subadults, i.e., individuals in dispersions, are present as well. This observation aligns with Palomares et al.[13] findings in extant *L. pardinus* populations from Doñana National Park (Coto del Rey, south-western Spain), where population composition typically ranges between 7 and 17 individuals, including 3 stable pairs of adults, their cubs and subadults in dispersion. It is also noteworthy that, according to taphonomic studies[53], lynxes were responsible for most of the leporid remains accumulated at the site (at least 221 individuals). Furthermore, the mortality profile of the lynx population shows a derived U-shaped curve in the histogram[66–68], and offers a snapshot of the ecosystem that comprised the Garraf Massif ~ 39.6 ka cal BP. The landscape of TC was predominantly an open environment, such as steppe, interspersed with distinct pine stands that likely formed a more extensive cover on the slopes of the nearby Garraf Massif. Additionally, thermophilus species associated with humid environments and riparian zones were present[53,69]. The Garraf Massif itself is a mountain range with rocky areas and cavities[70]. Although the *L. pardinus* today is restricted to a different ecosystem, it has been suggested that such environments may be favourable for *L. pardinus* ecology[23,27].

In contrast, the CG mortality profile consists of only 7 individuals, one more than previous identified[29]. However, there are significant differences in the geographical settings taphonomic context here. Cova del Gegant is a cave that was opened in front of a large-plain. Based on taphonomic analysis of fossil faunal remains, layer IIIa has been identified as an *L. pardinus* den[29]. The high accumulation of leporid remains, a high concentration of lynx-associated coprolites, and the presence of juvenile accumulated over time suggest that CG may have been used by *L. pardinus* to rear their cubs. In this study, we conducted the first in-depth ontogenetic analysis of cub remains, by applying the age categories presented here, which are based on behavioural milestones of this species. The results support the previous taphonomic study[29]. Stage A, which includes cubs of denning age, with sensory and locomotor capacities not fully developed preventing them from leaving the den[18,23], suggests that CG was used as a den by Upper Pleistocene *L. pardinus*. On the other hand, Stage D (individuals in the dispersal period, leaving their mother's territory) is not recorded. The lack of specimens at this stage makes sense if the cave was used primarily as a shelter for cubs. The presence of specimens in Stage C, categorized here as juveniles, may reflect young cubs following their mothers along camping routes and still using caves as shelter, but not denning. Finally, in Doñana, home to the largest current *L. pardinus* population, there are not caves, so the lynxes generally use hollow trunks or bushes to establish natal and auxiliary dens[23]. However, our results suggest that, in the past, this species used caves for breeding, as part of its reproductive ecology.

Both archaeological sites are located relatively close to each other (i.e., less than 30 km) and represent two distinct mortality profiles. TC is associated close to a living structure population, while CG is more aligned with a seasonal mortality profile. This interpretation is consistent with previous ones, which suggest that CG functioned as a lynx's den, whereas TC is closer to a riverside taphocenosis including denning episodes. This idea reinforces the notion that *L. pardinus* populations were adapted to different regional settings, including riverine landscapes in the case of TC and karstic environments in the case of CG, indicating the ecological plasticity of this species.

Based on our results, the methodologies proposed here could be used to assess cub survival viability in extant populations, which impacts in reproductive success and population growth rate[71]. Estimating the age at death of cubs, such as *L. pardinus*, provides insights into vulnerability factors in carnivores populations[32,72], offering valuable information for improving conservation tools, guiding scientific recommendations, adapting management and breeding strategies, and enhancing population sustainability[72–74].

The analysis of pulp cavity width offers an alternative to traditional methods for estimating age in fossil samples, such as dental eruption and replacement, counting visible *cementum annuli*, or observing wear in permanent teeth[36]. As with modern specimens, the results suggest that this method is suitable to classify *L. pardinus* fossil remains. In fossils, preservation is conditioned by taphonomic processes that occur during fossil-diagenesis. Sometimes, crowns may appear broken, or even the tooth root's apical foramen may be not present. In these cases, direct observations to classify specimens based on their developmental stage, can be challenging, and this methodology may help to avoid biases.

The age categories employed in this study have proven highly useful in identifying denning behaviour patterns in the fossil record of the *L. pardinus*. These categories primarily focus on juvenile individuals, which are among the key indicators of such activity in accumulation contexts[38,75–84]. Similarly, senile individuals also exhibit comparable patterns, but they are not considered in this study. For instance, in the spotted hyena, den sites are used by these individuals for resting and, ultimately, as places of death during the final stages of life[40].

This study does not aim to establish specific age categories for adult and senile individuals which is a limiting factor when attempting to reconstruct the MNI in Quaternary deposits. However, traditional adult age classifications in carnivorans are primarily based on dental wear[38,40,75,76,81], rather than on ontogenetic development. Although our results are consistent with our interpretation, it is important to acknowledge that future studies focusing on age categories for senile individuals will enhance the palaeoecological understanding of this species in the past.

Methods

A total of 39 hemimandibles and 31 maxillae of extant *L. pardinus* from the Estación Biológica de Doñana-CSIC (labelled "EBD") (Seville, Spain) and the Museo Nacional de Ciencias Naturales (MNCN) (Madrid, Spain) were studied. The material from EBD comprises 27 hemimandibles and 25 maxillae., of which 20 specimens are juveniles. Six of these specimens have known age at death, while 11 specimens provide a date of capture. The material originated from various locations in the southern Iberian Peninsula, including Córdoba, Huelva, Jaén, and Seville (Andalusia, Spain), Badajoz (Extremadura, Spain), and the Centro Nacional de Reprodução de Lince Ibérico (CNRLI) (Algarve, Portugal) (Supplementary Figure S2, Table S5). The material from the MNCN includes 12 hemimandibles and 6 maxillae, all of which belong to juveniles with no known age at death. These specimens were collected from Central Iberia (Los Yébenes and Peña Aguilera, Toledo, Spain) (Supplementary Figure S3, Table S6).

The *L. pardinus* fossil material was recovered from layer IIIa from Cova del Gegant (CG) (Sitges, Barcelona, Spain), and from Terrasses de la Riera dels Canyars (TC) (Gavà, Barcelona, Spain) as a result of the fieldwork conducted by the Grup de Recerca del Quaternari (GRQ-SERP, University of Barcelona, Spain). The fossils were processed, stored and identified at la Guixera laboratory (Castelldefels City Council) and at the university of Barcelona. Lynx remains from both sites have been previously published and cited in several papers[29,53,85,86]. The material analysed in this study from CG includes 11 cranial remains: 1 fragmented cranium, 1 maxilla, 6 hemimandibles, and 3 isolated carnassial teeth (Fig. 5; Table 4). The material from TC consists of 44 cranial remains: 2 crania, 10 maxillae, 22 hemimandibles, and 10 isolated carnassial teeth (Fig. 6; Table 4).

We adopt the terminology proposed by Hillson[86] to describe the dental elements in felids: dp_3-dp_4/DP^3-DP^4 for juveniles and p_3-p_4-m_1/P^3-P^4-M^1 for adult individuals. First, we developed an ontogenetic classification based on tooth development and replacement, upon which the prediction model is based. This classification aims to correlate distinct developmental stages with behavioural milestones of *L. pardinus*, facilitating its application to the fossil record. These classes are based on observations of dental development, eruption and replacement in juvenile and young adult individuals, obtained through X-rays. A total of 42 specimens were radiographed, resulting in 65 radiographs of 40 hemimandibles and 25 maxillae (Supplementary Table S5, S6). Digital radiographs of the specimens from the MNCN were performed at the Veterinary Hospital of the Complutense University of Madrid (Madrid, Spain), using a standard veterinary X-rays unit (Neovet, SEDECAL). Radiographs of the specimens from the EBD were carried out at the facilities of the aforementioned research centre, using a portable monoblock X-ray unit (Econet meX + 40 NPTH40-2002-014 series). Radiographs of the hemimandibles

Fig. 5. *Lynx pardinus* fossil material (Photographs by Israel Jimenez) from Cova del Gegant (CG) (Sitges, Barcelona, Spain). All hemimandibles are shown in labial view. (**a**) Left hemimandible (CG-4587 A); (**b**) Right hemimandible (CG-4587); (**c**) Cranium in lateral view (CG-4553); (**d**) Left hemimandible (CG-4574); (**e**) Right hemimandible (CG-4600); (**f**) Left hemimandible (CG-2810); (**g**) Right hemimandible (CG-6610).

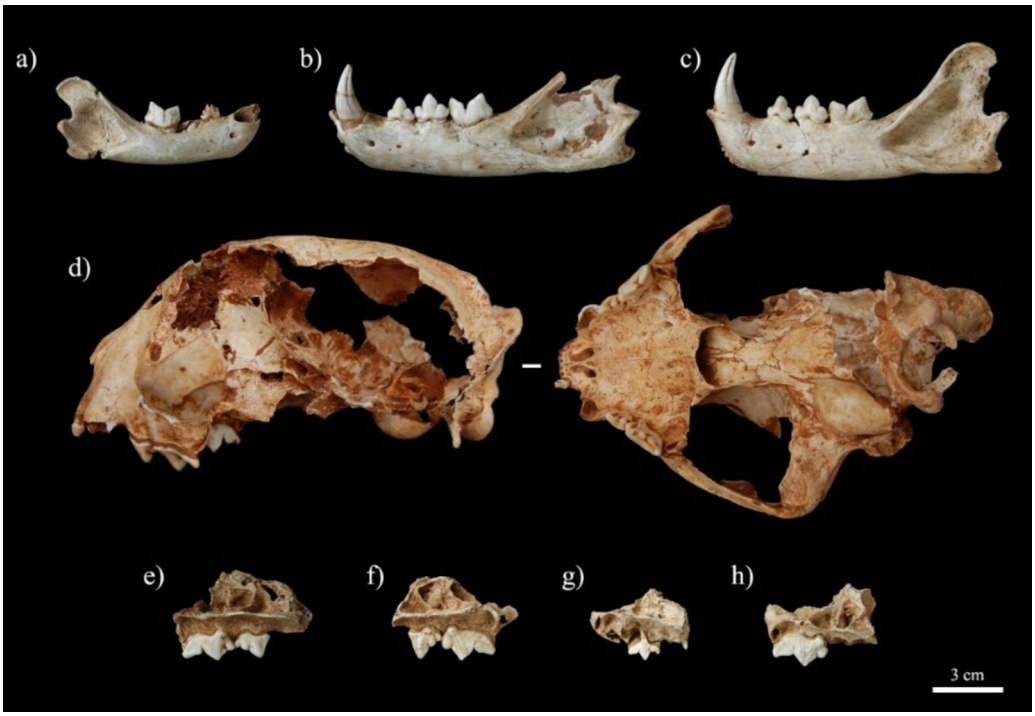

Fig. 6. *Lynx pardinus* fossil material ((Photographs by Israel Jimenez) from Terrasses de la Riera dels Canyars (TC) (Gavà, Barcelona, Spain). All hemimandibles are shown in labial view. (**a**) Left hemimandible (TC-4587 A); (**b**) Right hemimandible (TC-4587); (**c**) Cranium in lateral view (TC-4553); (**d**) Left hemimandible (TC-4574); (**e**) Right hemimandible (TC-4600); (**f**) Left hemimandible (TC-2810); (**g**) Right hemimandible (TC-6610).

were taken from a lateromedial projection whenever the condition of the specimen allowed. For the maxillae, to prevent the superimposition of bone tissues (e.g., the palate), which could hinder the visibility of the crown or the roots of the teeth, the maxillae were positioned at a 25º angle, if specimen condition permitted. Radiographs of the maxillae were taken from a mediolateral projection, as the specimens possessed complete skulls, which facilitated holding the specimen for the imaging proof.

The information of age of death of 6 juveniles individuals (EBD-25375 M: 4 weeks; EBD-29893 M: 4 months; EBD-29981 M: 1 month; EBD-29982 M: 2 months; EBD-30111 M: 7 months; EBD-30112 M: 6 months) (Supplementary Figure S2, S5, S6) was used as a reference to describe the ontogenetic stages. To support our observations, we relied on previous descriptions by other authors concerning the juvenile development of *L. pardinus*. García-Perea[41] describes the dental replacement process in the genus *Lynx*. Yerga[18] and Yerga et al.[42] describe the early development and growth of cubs during their first month of life. Regarding to young adults, our observations were supported by Zapata et al.[21] which determine the age of *L. pardinus* using canine root radiographs and cementum annuli enumeration. To strengthen the classification, as the number of specimens with known age is limited and does not cover the full range of postnatal development (from birth to sexual maturity), we compare our observations and previous studies about *L. pardinus* development from other species of the genus *Lynx*. As for example *Lynx rufus*[55] or *Lynx lynx*[57].

Following our analysis of lynx collections from EBD and MNCN, as well as descriptions of *Lynx* development by previous authors[18,21,23,42], we applied 5 ontogenetic stages based on tooth development and dental replacement (Fig. 1). These stages cover from new born to adult (sexual maturity). The categories, ordered by age range, are as follows:

- Stage A: Birth to 2 months old. New born or infantile. This stage spans the development of deciduous cheek teeth to the completion of the eruption. Teeth eruption begins around the third week of life, starting with the canines and incisors and ending with the premolars, at approximately 40 days old[23]. At this stage, all deciduous teeth erupted (dp_3-dp_4/DP^3-DP^4) have, but the apices of the roots remain open and under development. The pulp chambers of all deciduous cheek teeth are immature. The crowns of the permanent carnassial teeth (m_1 and P^4 begin to develop and are visible in the alveolar sacs. The enamel does not extend to the interarticular bifurcation, leaving the cementum-enamel junction unformed. The crowns of the permanent premolars (p_3-p_4/P^3) also start to form, appearing as calcification points in the alveolar sacs. Canine teeth appear to develop at the same time as the carnassial teeth.
- Stage B: From 2 months to 5 months old. Juvenile. This stage encompasses the eruption of the carnassial teeth (m_1 and P^4 and the continued development of the crowns of the permanent premolars. The roots of the deciduous premolars are closed. The crowns of the upper and lower premolars show advanced stage of devel-

opment, with some specimens exhibiting fully formed crowns extending to the cementum-enamel junction. The horns of the pulp chambers remain in development, presenting an umbrella-like shaped at their tips. The crown of the carnassial teeth is formed down to the enamel-junction, with the interarticular bifurcation fully calcified and root elongation initiated. The cementum on the roots is still relatively thick. At this stage, root length may be shorter or equal to crown height.

- Stage C: From 5 months to 10 months old. Juvenile. This stage marks the replacement of deciduous premolars by permanent ones (dp_3-dp_4/DP^3-DP^4 by p_3-p_4-m_1/P^3-P^4-M^1). The roots of the deciduous premolars display signs of resorption, while the roots of p_3-p_4/P^3 vary in length, being shorter, equal to, or longer than the crown height, depending on the progression of eruption. The roots of the carnassial teeth have reached their full length, now longer than the crown height. Although the pulp chambers remain immature and dentine beneath the enamel continues, the alveolar bone of m_1 and P^4 nears the gingival surface, signalling the final stages of tooth eruption. At this point, root apices remain open.
- Stage D: From 10 to 18 months old. Subadult. This stage is characterised by the closure of the open apices in the roots of permanent teeth. The pulp chambers of all permanent teeth approach maturity, adopting an isosceles triangle shape in the main cusps of the premolars and in the paracone/paraconid and metacone/metaconid horns of the carnassial teeth. The root apices are almost completely closed. According to Zapata et al.[21] closure of the apical foramen of canine occurs at 12 to 18 months of age.
- Stage E: Older than 18 months old. Adult. At this stage, the pulp chambers of the permanent teeth reach full maturity, and the roots are completely closed.

We followed the methodology proposed by Nomokonova et al.[47], which analyse the infilling of pulp cavities in the roots of molars and premolars in dogs from archaeological contexts. We used the root of the upper fourth premolar (P^4 and the lower first molar (m_1). For P^4, we analysed the distal root due to its greater thickness. The mesial and lingual roots were discarded because the latter overlapped the former in mediolateral projections. For m_1, we independently analysed the distal and mesial thickness of the root. To measure the width of the root and pulp cavity (in millimetres), we use the software Radiant Dicom Viewer (Medixant. RadiAnt DICOM Viewer, Version 2021.1. Jun 27, 2021. URL: https://www.radiantviewer.com). Measurements were taken at the midpoints between the junction of mesial and distal roots and the ends of the roots, ensuring a 90-degree angle to the pulp cavity margin (see Fig. 3 in Nomokonova et al.[47]. Pulp cavity closure ratios were calculated by dividing pulp cavity widths by the total root widths. To visually inspect the relationship between the pulp cavity indexes and age categories in modern lynxes, we generated box plots for each analysed root. To assess the strength of the relationship between the indexes and age categories, we used Pearson's correlation, which relates a categorical variable (stages) and another numerical variable (indexes). Statistical analyses were conducted using the free-use statistical software Past3: Paleontological Statistics Software Package for Education and Data Analysis[88]. We then developed a predictive age model (based on extant sample data) to be applied to independent samples. The analysis was carried out using the statistical software R (Version 4.4.1. URL: https://www.R-project.org/).

To generate the ordinal logistic model, we used the R package "Glm2", which includes the function "polr(formula = y ~ x, data = a, Hess = TRUE)". In this function, "*y*" represents the dependent variable (stage), and "*x*" represents the independent variable (index) Through this function, we obtained the coefficient and intercept which were used to obtain the critical values required to determine the transition between developmental stage. The software also provides the option to apply this equation across all categories. To achieve this, we instructed it to execute the "predict(b)" function, where *b* represents the model. Finally, to observe the numerical probability of an index belonging to each stage, we performed a fitted probabilities calculation using the "fitted(b)" function. This approach allowed us to evaluate the effectiveness of the method. The model was subsequently applied to the indexes obtained from fossils sample from TC and CG sites. Minimum, maximum, medians, standard error (SE) and standard deviation (SD) were calculated for each stage (see supplementary Table S1).

To analyse fossil samples, we first classified the specimens using the age categories proposed in this work. Then, the equation predictions were applied to enhance the model's performance. The indexes were obtained through radiography, followings the same methodology as for the extant specimens. The X-ray imaging technique was carried out at two different facilities. A total of 40 specimens were radiographed: 14 specimens from TC at the Veterinary Hospital of the Complutense University of Madrid, and 14 specimens from TC as along with 12 specimens from CG at a private veterinary clinic (Clínica Veteralia Diagonal) located in Castelldefels (Barcelona, Spain) (see supplementary Material). The Number of Identified Specimens (NISP) and the Minimum Number of Individuals (MNI) were calculated to develop the mortality profile for each age category. The MNI was calculated using the permanent lower and upper carnassial teeth (m_1 and P^4 and deciduous dp_4 and DP^3 (Table 4). Cranial samples (teeth within mandibles and maxillae) were divided into right/left and upper/lower elements. After obtaining the MNI for each set, isolated teeth were incorporated to avoid counting double-counting individuals. Permanent teeth in development, such as forming crowns or growing roots, were classified as juvenile remains. Once the MNI was calculated for both TC and CG lynx populations, their age structure was represented as histogram to discuss its palaeocological implications.

Data availability

Data is provided within the manuscript or supplementary information.

Received: 29 November 2024; Accepted: 25 April 2025
Published online: 13 May 2025

References

1. Rodríguez, A. & Calzada, J. *Lynx pardinus. IUCN Red List. Threatened Species* **2015**, e.T12520A50655794.
2. Guzmán, J. et al. *El Lince Ibérico (Lynx pardinus) En España Y Portugal. Censo Diagnóstico De sus Poblaciones* (Dirección General para la Biodiversidad, 2004).
3. MITECO, I. C. N. F. *Censo De Lince Ibérico* (MITECO, 2022).
4. Cisneros-Araujo, P. et al. Born to be wild: Captive-born and wild *L. pardinus* (*Lynx pardinus*) reveal space-use similarities when reintroduced for species conservation concerns. *Biol. Conserv.* **294**, 110646. https://doi.org/10.1016/j.biocon.2024.110646 (2024).
5. Mecozzi, B. et al. The Tale of a short-tailed Cat: new outstanding late pleistocene fossils of *Lynx pardinus* from Southern Italy. *Quat Sci. Rev.* **262**, 106840. https://doi.org/10.1016/j.quascirev.2021.106840 (2021).
6. Rodríguez-Varela, R. et al. Ancient DNA evidence of *L. pardinus* palaeoendemism. *Quat Sci. Rev.* **112**, 172–180. https://doi.org/10.1016/j.quascirev.2015.01.009 (2015).
7. Villaluenga, A. Biogeographic analysis of Upper Pleistocene felid (*Felis, Lynx* and *Panthera*) remains in archaeological sites on the Iberian Peninsula. In *The Homotherium Finds from Schöningen 13II-4: Man and Big Cats of the Ice Age* (eds. Conard, N. J., Henning, H., Kurt, H., Jordi, S. & Thomas, T.) (Mainz, 2022).
8. Ferreras, P., Beltrán, J. F., Aldama, J. J. & Delibes, M. Spatial organization and land tenure system of the endangered *L. pardinus* (*Lynx pardinus*). *J. Zool.* **243**, 163–189. https://doi.org/10.1111/j.1469-7998.1997.tb05762.x (1997).
9. Rodríguez, A. *Lynx pardinus* Temminck, 1827. In *Atlas y Libro Rojo de los Mamíferos Terrestres de España* (eds. Palomo, L., Gisbert, J. & Blanco, J.) 342–344 (Dirección General para la Biodiversidad - SECEM-SECEMU, 2007).
10. Beltrán, J. & Delibes, M. Physical characteristics of *L. pardinus* (*Lynx pardinus*) from Doñana, Southwestern Spain. *J. Mammal.* **74**, 852–862. https://doi.org/10.2307/1382423 (1993).
11. Calzada, S. *Impacto De Depredación Y Selección De Presa Del Lince Ibérico Y El Zorro Sobre El Conejo* (Universidad de León, 2000).
12. Delibes, M. Feeding ecology of the Spanish lynx in the Coto Doñana. *Acta Theriol.* **25**, 309–324 (1980).
13. Palomares, F. et al. Spatial ecology of *L. pardinus* and abundance of European rabbits in Southwestern Spain. *Wildl. Monogr.* 1–36. https://www.jstor.org/stable/3830752 (2001).
14. Aldama, J. *Ecología Energética Y Reproductiva Del Lince Ibérico (Lynx Pardinus Temminck, 1824) En Doñana* (Universidad Complutense de Madrid, 1993).
15. Gaona, P., Ferreras, P. & Delibes, M. Dynamics and viability of a metapopulation of the endangered *L. pardinus* (*Lynx pardinus*). *Ecol. Monogr.* **68**, 349–370. https://doi.org/10.1890/0012-9615(1998)068[0349:DAVOAM]2.0.CO;2 (1998).
16. Ferreras, P. et al. Proximate and ultimate causes of dispersal in the *L. pardinus* (*Lynx pardinus*). *Behav. Ecol.* **15**, 31–40. https://doi.org/10.1093/beheco/arg097 (2004).
17. Vargas, A. et al. Interdisciplinary methods in the *L. pardinus* (*Lynx pardinus*) conservation breeding programme. In I Curso De Cría En Cautividad De Especies Ibéricas Amenazadas: Conservación ex-situ (Facultad de Veterinaria de León, 2009).
18. Yerga, J. *Ontogenia Del Comportamiento Del Lince Ibérico (Lynx pardinus) En Cautividad* (Universidad de Huelva, 2016).
19. Palomares, F. Reproduction and pre-dispersal survival of *L. pardinus* in a subpopulation of the Doñana National park. *Biol. Conserv.* **122**, 53–59. https://doi.org/10.1016/j.biocon.2004.06.020 (2005).
20. Fernández, N., Palomares, F. & Delibes, M. The use of breeding dens and kitten development in the *L. pardinus* (*Lynx pardinus*). *J. Zool.* **258**, 1–5. https://doi.org/10.1017/S0952836902001140 (2002).
21. Zapata, S. C. et al. Age determination of *L. pardinus* (*Lynx pardinus*) using canine radiograph and cementum annuli enumeration. *Z. Säugetierkd.* **62**, 119–123 (1997).
22. Engebretsen, K. N., Rushing, C., DeBloois, D. & Young, J. K. Increased maternal care improves neonate survival in a solitary carnivore. *Anim. Behav.* **210**, 369–381. https://doi.org/10.1016/j.anbehav.2024.01.012 (2024).
23. Fernández, N. & Palomares, F. The selection of breeding dens by the endangered *L. pardinus* (*Lynx pardinus*): Implications for its conservation. *Biol. Conserv.* **94**, 51–61. https://doi.org/10.1016/S0006-3207(99)00164-0 (2000).
24. Pruss, S. Selection of natal dens by the swift fox (*Vulpes velox*) on the Canadian prairies. *Can. J. Zool.* 77, 646–652. https://doi.org/10.1139/z99-001 (1999).
25. Ross, S., Kamnitzer, R., Munkhtsog, B. & Harris, S. Den-site selection is critical for Pallas's cats (*Otocolobus manul*). *Can. J. Zool.* 88, 905–913. https://doi.org/10.1139/Z10-056 (2010).
26. Ruggiero, L., Pearson, E. & Henry, S. Characteristics of American Marten Den sites in Wyoming. *J. Wildl. Manage.* **62**, 663–673. https://www.jstor.org/stable/3802342 (1998).
27. Fernández, N., Delibes, M. & Palomares, F. Landscape evaluation in conservation: molecular sampling and habitat modelling for the *L. pardinus*. *Ecol. Appl.* **16**, 1037–1049. https://doi.org/10.1890/1051-0761(2006)016[1037:LEICMS]2.0.CO;2 (2006).
28. Gabucio, M. J., Sanz, M. & Daura, J. Lynxes and foxes among hyenas, bears and humans. Unit 3 of the Cova Del coll Verdaguer upper pleistocene site (Barcelona, Iberian Peninsula). *Quat Sci. Rev.* **333**, 108671. https://doi.org/10.1016/j.quascirev.2024.108671 (2024).
29. Rodríguez-Hidalgo, A., Sanz, M., Daura, J. & Sánchez-Marco, A. Taphonomic criteria for identifying *L. pardinus* dens in quaternary deposits. *Sci. Rep.* **10**, 7225. https://doi.org/10.1038/s41598-020-63908-6 (2020).
30. Sanz, M. & Daura, J. Carnivore involvement in bone assemblages based on taphonomic and Zooarchaeological analyses of Cova Del coll Verdaguer site (Barcelona, Iberian Peninsula). *Hist. Biol.* **30**, 807–820. https://doi.org/10.1080/08912963.2017.1351561 (2018).
31. Sanz, M., Daura, J., Égüez, N. & Brugal, J. P. Not only hyenids: A multi-scale analysis of upper pleistocene carnivore coprolites in Cova Del coll Verdaguer (NE Iberian Peninsula). *Palaeogeogr Palaeoclimatol Palaeoecol.* **443**, 249–262. https://doi.org/10.1016/j.palaeo.2015.11.047 (2016).
32. Karanth, K. U. Tiger ecology and conservation in the Indian Subcontinent. *J. Bombay Nat. Hist. Soc.* **100**, 169–189 (2003).
33. Kerley, L. L. et al. Reproductive parameters of wild female Amur (Siberian) Tigers (*Panthera Tigris altaica*). *J. Mammal.* **84**, 288–298. (2003).
34. Krebs, C. J. *Ecological Methodology* (Addison-Wesley, 1999).
35. Mbizah, M. M., Steenkamp, G. & Groom, R. J. Evaluation of the applicability of different age determination methods for estimating age of the endangered African wild dog (*Lycaon pictus*). *PLoS One.* **11**, e0164676. https://doi.org/10.1371/journal.pone.0164676 (2016).
36. Klein, R. G., Wolf, C., Freeman, L. G. & Allwarden, K. The use of dental crown heights for constructing age profiles of red deer and similar species in archaeological samples. *J. Archaeol. Sci.* **8**, 1–31. https://doi.org/10.1016/0305-4403(81)90010-8 (1981).
37. Spinage, C. A. A review of the age determination of mammals by means of teeth, with especial reference to Africa. *Afr. J. Ecol.* **11**, 165–187 (1973).
38. Cardoso, H. F. Epiphyseal union at the innominate and lower limb in a modern Portuguese skeletal sample, and age Estimation in adolescent and young adult male and female skeletons. *Am. J. Phys. Anthropol.* **135**, 161–170. https://doi.org/10.1002/ajpa.20717 (2008).
39. Jimenez, I. J. et al. Ontogenetic dental patterns in pleistocene hyenas (*Crocuta crocuta* Erxleben, 1777) and their Palaeobiological implications. *Int. J. Osteoarchaeol.* **29**, 808–821. https://doi.org/10.1002/oa.2796 (2019).
40. Jimenez, I. J. et al. Society of the Den: identifying patterns of Denning behaviour in upper pleistocene hyena populations. *Quat Sci. Rev.* **345**, 109004. https://doi.org/10.1016/j.quascirev.2024.109004 (2024).
41. Garcia-Perea, R. Patterns of postnatal development in skulls of lynxes, genus Lynx (Mammalia: Carnivora). *J. Morphol.* **229**, 241–254. (1996).

42. Yerga, J. et al. Early development and growth in captive-born *L. pardinus* (*Lynx pardinus*). *Zoo Biol.* **33**, 381–387. https://doi.org/10.1002/zoo.21148 (2014).
43. Kershaw, K., Allen, L., Lisle, A. & Withers, K. Determining the age of adult wild dogs (*Canis L.pus dingo*, *C. L. domesticus* and their hybrids). I. Pulp cavity: tooth width ratios. *Wildl. Res.* **32**, 581–585. https://doi.org/10.1071/WR03109 (2005).
44. Knowlton, F. F. & Whittemore, S. L. Pulp cavity-tooth width ratios from known-age and wild-caught Coyotes determined by radiography. *Wildl. Soc. Bull.* 239–244. https://www.jstor.org/stable/3784003 (2001).
45. Landon, D. B., Waite, C. A., Peterson, R. O. & Mech, L. D. Evaluation of age determination techniques for Gray wolves. *J. Wildl. Manage.* 674–682. https://www.jstor.org/stable/3802343 (1998).
46. Meihls, M. L. *Age Determination of Domesticated Dogs Using Pulp Chamber To Tooth Width Ratio* (Ohio Dominican University, 2018).
47. Nomokonova, T. et al. Age Estimation of archaeological dogs using pulp cavity closure ratios. *J. Archaeol. Sci.* **123**, 105252. https://doi.org/10.1016/j.jas.2020.105252 (2020).
48. Smirnov, V. S., Korytin, N. S. & Neganov, V. G. Kontrol'za dinamikoi chislennosti volka po vozrastnomu sostavu doby-vaemykh zhivotnykh (1985).
49. Smirnov, V. S. Issledovanie Dinamiki chislennosti Volka s Ispol'zovaniem Dvukh Metodov Opredeliniia Vozrasta. In Analiz Vozrastnoi Struktury Populiatsii Pozvonochnykh (ed Bezel', V. S.) (UrO AN SSSR, (1988).
50. Stefen, C. Testing pulp cavity closure to estimate individual age of *Felis silvestris* (Carnivora: Felidae). *Lynx Ser. Nova* 46 (2015).
51. Thomson, P. C. & Rose, K. Age determination of Dingoes from characteristics of canine teeth. *Wildl. Res.* **19**, 597–599. https://doi.org/10.1071/WR9920597 (1992).
52. Tumilson, R. & McDaniel, V. R. Gray Fox age classification by canine tooth pulp cavity radiographs. *J. Wildl. Manage.* **48**, 228–230 (1984). https://www.jstor.org/stable/3808477
53. Daura, J. et al. Terrasses de La Riera Dels Canyars (Gavà, Barcelona): the Landscape of Heinrich stadial 4 North of the Ebro frontier and implications for modern human dispersal into Iberia. *Quat Sci. Rev.* **60**, 26–48. https://doi.org/10.1016/j.quascirev.2012.10.042 (2013).
54. Steele, T. E. & Weaver, T. D. The modified triangular graph: A refined method for comparing mortality profiles in archaeological samples. *J. Archaeol. Sci.* **29**, 317–322. https://doi.org/10.1006/jasc.2001.0733 (2002).
55. Steele, T. E. Using mortality profiles to infer behavior in the fossil record. *J. Mammal.* **84**, 418–430. (2003).
56. Segura, V. A three-dimensional skull ontogeny in the bobcat (*Lynx rufus*) (Carnivora: Felidae): A comparison with other carnivores. *Can. J. Zool.* **93**, 225–237. https://doi.org/10.1139/cjz-2014-0148 (2015).
57. Martí, I. & Ryser-Degiorgis, M. P. A tooth wear scoring scheme for age Estimation of the Eurasian lynx (*Lynx lynx*) under field conditions. *Eur. J. Wildl. Res.* **64**, 1–13. https://doi.org/10.1007/s10344-018-1198-6 (2018).
58. Marks, S. A. & Erickson, A. W. Age determination in the black bear. *J. Wildl. Manage.* **30**, 389–410 (1966). https://www.jstor.org/stable/3797827
59. Binder, W. J., Thompson, E. N. & Van Valkenburgh, B. Temporal variation in tooth fracture among rancho La Brea dire wolves. *J. Vertebr Paleontol.* **22**, 423–428. https://doi.org/10.1671/0272-4634(2002)022[(2002). 0423:TVITFA]2.0.CO;2.
60. Smith, B. & Vague, A. L. The Denning behaviour of Dingoes (*Canis dingo*) living in a human-modified environment. *Aust Mammal.* **39**, 161–168. https://doi.org/10.1071/AM16027 (2016).
61. Trapp, J. R., Beier, P., Mack, C., Parsons, D. R. & Paquet, P. C. Wolf (*Canis lupus*) Den site selection in the Rocky mountains. *Can. Field-Nat.* **122**, 49–56. https://doi.org/10.22621/cfn.v122i1.543 (2008).
62. Hewson, R. The use of dens by hill foxes (*Vulpes vulpes*). *J. Zool.* **233**, 331–335. https://doi.org/10.1111/j.1469-7998.1994.tb08596.x (1994).
63. Boutros, D. et al. Characterisation of Eurasian lynx (*Lynx lynx*) Den sites and kitten survival. *Wildl. Biol.* **13**, 417–429. https://doi.org/10.2981/0909-6396(2007)13[417:COELLL]2.0.CO;2 (2007).
64. Sorum, M. S. et al. Den-site characteristics and selection by brown bears (*Ursus arctos*) in the central Brooks Range of Alaska. *Ecosphere* 10, e02822. https://doi.org/10.1002/ecs2.2822 (2019).
65. Rosado-Méndez, N. Y., Lloveras, L., Daura, J., Nadal, J. & Sanz, M. Predator agents and leporid accumulations: the case of terrasses de La Riera Dels Canyars (Gavà, Barcelona, Spain). *J. Archaeol. Method Theory*. **22**, 980–1005. https://doi.org/10.1007/s10816-014-9214-y (2015).
66. Klein, R. G. Age (mortality) profiles as a means of distinguishing hunted species from scavenged ones in stone age archeological sites. *Paleobiology* **8**, 151–158. https://doi.org/10.1017/S0094837300004498 (1982).
67. Lyman, R. L. On the analysis of vertebrate mortality profiles: sample size, mortality type, and hunting pressure. *Am. Antiq.* **52**, 125–142. https://doi.org/10.2307/281064 (1987).
68. Stiner, M. C. The use of mortality patterns in archaeological studies of hominid predatory adaptations. *J. Anthropol. Archaeol.* **9**, 305–351. https://doi.org/10.1016/0278-4165(90)90010-B (1990).
69. López-García, J. M., Blain, H. A., Bennàsar, M., Sanz, M. & Daura, J. Heinrich event 4 characterized by terrestrial proxies in Southwestern Europe. *Clim. Past*. **9**, 1053–1064. https://doi.org/10.5194/cp-9-1053-2013 (2013).
70. Daura, J., Sanz, M., Fornós, J. J. & Asensio, A. Julià Brugués, R. Karst evolution of the Garraf Massif (Barcelona, Spain): doline formation, chronology and Archaeopalaeontological archives. *Quat Int.* **331**, 44–57. https://doi.org/10.4311/2011ES0254 (2014).
71. Owen, C., Niemann, S. & Slotow, R. Copulatory parameters and reproductive success of wild leopards in South Africa. *J. Mammal.* **91**, 1178–1187. https://doi.org/10.1644/09-MAMM-A-256.1 (2010).
72. Planella, A. et al. Integrating critical periods for bear Cub survival into Temporal regulations of human activities. *Biol. Conserv.* **236**, 489–495. https://doi.org/10.1016/j.biocon.2019.05.051 (2019).
73. Linnell, J. D. C. et al. Home range size and choice of management strategy for lynx in Scandinavia. *Environ. Manage.* **27**, 869–879. https://doi.org/10.1007/s002670010195 (2001).
74. Saunders, S. P., Harris, T., Traylor-Holzer, K. & Beck, K. G. Factors influencing breeding success, ovarian Cyclicity, and Cub survival in zoo-managed Tigers (*Panthera tigris*). *Anim. Reprod. Sci.* **144**, 38–47. https://doi.org/10.1016/j.anireprosci.2013.11.006 (2014).
75. Brugal, J. P., Fosse, P. & Guadelli, J. L. Comparative study of bone assemblages made by recent and Pleistocene Hyenids. *Proc. 1993 Bone Modif. Conf., Hot Springs, South Dakota, Archaeol. Lab., Augustana Coll., Sioux Falls, Occas. Publ.* 158, 158–187 (1997).
76. Fourvel, J. B. Hyénidés modernes et fossiles d'Europe et d'Afrique: taphonomie comparée de leurs assemblages osseux. *Archéologie et Préhistoire*, Université Toulouse le Mirail - Toulouse II. NNT: 2012TOU20145 (2012).
77. Kuhn, B. F., Berger, L. R. & Skinner, J. D. Examining criteria for identifying and differentiating fossil faunal assemblages accumulated by hyenas and hominins using extant hyenid accumulations. *Int. J. Osteoarchaeol.* **20**, 15–35. https://doi.org/10.1002/oa.996 (2010).
78. Lansing, S. W., Cooper, S. M., Boydston, E. E. & Holekamp, K. E. Taphonomic and Zooarchaeological implications of spotted hyena (*Crocuta crocuta*) bone accumulations in Kenya: a modern behavioral ecological approach. *Paleobiology* **35**, 289–309. https://doi.org/10.1666/08009.1 (2009).
79. Pickering, T. R. Reconsideration of criteria for differentiating faunal assemblages accumulated by hyenas and hominids. *Int. J. Osteoarchaeol.* **12**, 127–141. https://doi.org/10.1002/oa.594 (2002).
80. Stiner, M. C. The faunal remains from Grotta Guattari: a taphonomic perspective. *Curr. Anthropol.* **32**, 103–117 (1991).
81. Stiner, M. C. *Honor among Thieves: A Zooarchaeological Study of Neandertal Ecology* (Princeton Univ. Press, 1994).

82. Stiner, M. C. Comparative ecology and taphonomy of spotted hyenas, humans, and wolves in pleistocene Italy. *Rev. Paléobiol.* **23**, 771–785 (2004).
83. Villa, P., Castel, J. C., Beauval, C., Bourdillat, V. & Goldberg, P. Human and carnivore sites in the European middle and upper paleolithic: similarities and differences in bone modification and fragmentation. *Rev. Paléobiol.* **23**, 705–730 (2004).
84. Villa, P. et al. The archaeology and paleoenvironment of an upper pleistocene hyena Den: an integrated approach. *J. Archaeol. Sci.* **37**, 919–935. https://doi.org/10.1016/j.jas.2009.11.025 (2010).
85. Sanz, M. *Patrons D'acumulació De Restes De Fauna Del Plistocè Superior Al nord-est Peninsular (àrea Del Massís Del Garraf-Ordal)* (Universidad de Barcelona, 2013).
86. Sanz, M., Daura, J., Égüez, N. & Cabanes, D. On the track of anthropogenic activity in carnivore dens: altered combustion structures in Cova Del Gegant (NE Iberian Peninsula). *Quat Int.* **437**, 102–114. https://doi.org/10.1016/j.quaint.2015.10.057 (2017).
87. Hillson, S. *Teeth* (Cambridge University Press, 1986).
88. Hammer, Ø., Harper, D. *Paleontological Data Analysis.* (Wiley, 2024).

Acknowledgements

This research was supported by the PhD scholarship "Training of researchers UCM Program" of the Universidad Complutense de Madrid; by the UCM research group Ecosistemas Cuaternarios (931098); by the project "Geología, geocronología y paleobiología de los yacimientos de la Sierra de Atapuerca VIII" (PID2021-122355NB-C31- FEDER/Ministerio de Ciencia e Innovación, Agencia Estatal); by Ramon y Cajal postdoctoral grant (RYC2021-032999-I, M.S.) with financial sponsorship of Ministerio de Ciencia e Innovación and the European Union NextGenerationEU; the Departament de Cultura de la Generalitat de Catalunya (grant no. CLT/2022/ARQ001SOLC/128) and AGAUR (SGR2021-00337); Ministerio de Ciencia e Innovación government of Spain (PID2020-113960GB-100/AEI/10.13039/501100011033). We want to thank the technical staff from the X-ray service of Servicio de Diagnóstico por Imagen del Hospital Clínico Veterinario Complutense. We want to thank Ángel Garvia (Mammal Curator of Museo Nacional de Ciencias Naturales de Madrid), and Carlos Urdiales (Vertebrate Collections Curator of Estación Biológica de Doñana) for the assistance and access to extant Iberian lynx specimens. We also want to thank Jaime Goyoaga (Jaime Goyoaga S.L.P. Equine Clinic) for carried out X-rays on extant specimens of Iberian lynx at the Estación Biológica de Doñana, and Joan RamónCesari (Clínica Veterinària Diagonal Castelldefels) for carried out X-rays on fossils specimens from CG and TC. Last, we thank the Castelldefels City Council (La Guixera Laboratory) where the fossils are curated.

Author contributions

All authors have contributed to the realization of this work. I.J.J. was responsible for visualising and conceptualising the work, investigation, methodology, formal analysis, written and editing the original draft. R.G.G. was responsible of development of methodology and formal analysis, writing and editing the original draft. M.S. and J.D. were responsible of resources providing study fossils materials and archaeological context, written and edited the original draft. I.d.G. and M.I.G.R. assumed management and coordination responsibility for the research activity planning and execution of all the specimens and also edited the original draft. N.G. has supervised the investigation, project administration, written and edited the original draft. All authors have read, corrected and approved the final version of the manuscript.

Declarations

Competing interests

The authors declare no competing interests.

Declaration of generative AI and AI-assisted technologies in the writing process

During the preparation of this work the author(s) used ChatGPT in order to improve language and readability. After using this tool/service, the author(s) reviewed and edited the content as needed and take(s) full responsibility for the content of the publication.

Additional information

Supplementary Information The online version contains supplementary material available at https://doi.org/10.1038/s41598-025-00229-6.

Correspondence and requests for materials should be addressed to N.G.